

## Article

# Identification of a Possible Endocannabinoid-Mediated Mechanism of Action of Cetylated Fatty Acids

Giulia Bononi <sup>1,2</sup> , Carlotta Granchi <sup>1,2</sup> , Tiziano Tuccinardi <sup>1,2</sup>  and Filippo Minutolo <sup>1,2,\*</sup> 

<sup>1</sup> Department of Pharmacy, University of Pisa, Via Bonanno 6, 56126 Pisa, Italy; giulia.bononi@unipi.it (G.B.); carlotta.granchi@unipi.it (C.G.); tiziano.tuccinardi@unipi.it (T.T.)

<sup>2</sup> Center for Instrument Sharing of the University of Pisa (CISUP), Lungarno Pacinotti 43, 56126 Pisa, Italy

\* Correspondence: filippo.minutolo@unipi.it

**Abstract:** Some musculoskeletal disorders, including osteoarthritis; arthrosis; post-traumatic injuries; and other inflammatory tendon, joint and muscular afflictions, still represent unmet medical needs. Cetylated fatty acids (CFAs) are key components of widely distributed over-the-counter products, especially for topical use, which are intended to reduce symptoms associated with these conditions. Nevertheless, the mechanism of action of CFAs' analgesic and anti-inflammatory properties has not yet been clearly established. Endocannabinoids, such as 2-arachidonoylglycerol (2-AG) and anandamide (AEA), are known to produce analgesic and anti-inflammatory effects. These compounds undergo physiological inactivation operated by several enzymes, including monoacylglycerol lipase (MAGL). We herein demonstrate for the first time that the therapeutic effects of CFAs may be attributable, at least in part, to their MAGL inhibition activities, which induce a local increase in analgesic/anti-inflammatory endocannabinoids in close proximity to the site of administration. These findings pave the way for the development of new potent local analgesic agents, whose action is based on an indirect cannabinoid effect.

**Keywords:** endocannabinoid system; cetylated fatty acids; monoacylglycerol lipase; MAGL inhibitors; analgesic agents; anti-inflammatory agents



Academic Editor: Balapal  
S. Basavarajappa

Received: 12 February 2025

Revised: 25 February 2025

Accepted: 1 March 2025

Published: 2 March 2025

**Citation:** Bononi, G.; Granchi, C.; Tuccinardi, T.; Minutolo, F. Identification of a Possible Endocannabinoid-Mediated Mechanism of Action of Cetylated Fatty Acids. *Biomolecules* **2025**, *15*, 363. <https://doi.org/10.3390/biom15030363>

**Copyright:** © 2025 by the authors. Licensee MDPI, Basel, Switzerland. This article is an open access article distributed under the terms and conditions of the Creative Commons Attribution (CC BY) license (<https://creativecommons.org/licenses/by/4.0/>).

## 1. Introduction

Musculoskeletal disorders, including osteoarthritis, tendinitis, and various forms of soft tissue inflammation, represent a significant burden on global health. These conditions often lead to chronic pain, reduced mobility, and a diminished quality of life. Conventional treatments for musculoskeletal pathologies typically involve the use of nonsteroidal anti-inflammatory drugs (NSAIDs), corticosteroids, and physical therapy. However, these approaches can be associated with a range of side effects and limitations, prompting the need for alternative therapeutic strategies [1].

Cetylated fatty acids (CFAs) have emerged as a promising class of compounds in the management of musculoskeletal disorders, demonstrating anti-inflammatory and pain-relieving properties. The most renowned CFA is cetyl myristoleate, also known as CMO (Figure 1), which was first identified for its potential in treating arthritis [2]. From a molecular perspective, CFAs are naturally occurring lipophilic esters derived from plant and/or animal sources, consisting of fatty acids esterified with cetyl alcohol (possessing a linear saturated C16 alkyl chain). In addition to the aforementioned CMO, this series of compounds generally includes other analogues such as cetyl myristate, cetyl palmitoleate, cetyl palmitate, cetyl oleate, and cetyl laurate (Figure 1) [3,4].

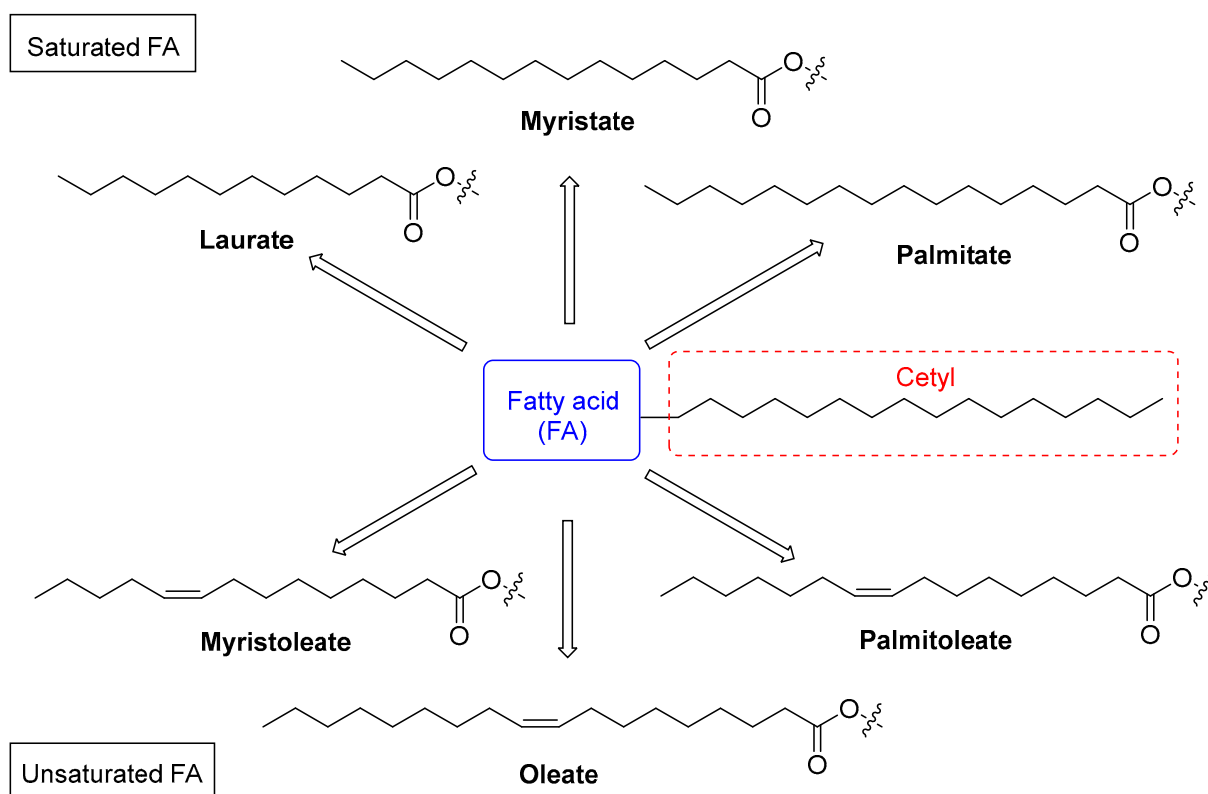


**Figure 1.** Some representative examples of naturally occurring CFAs, both saturated and unsaturated, present in most topical preparations for the treatment of musculoskeletal disorders. The common cetyl portion is highlighted in the red dashed square.

CFAs are commonly administered topically due to their rapid absorption via passive permeation through cell membranes, facilitated by their lipid nature [5]. They are primarily used in therapy for their anti-inflammatory and analgesic properties, particularly in the management of joint pain, inflammation, and muscle recovery, as well as for improving joint mobility in conditions such as osteoarthritis and rheumatoid arthritis [3,6–9]. Recent studies have demonstrated the efficacy of topical CFAs in treating symptoms associated with athletic pubalgia in professional roller hockey players [10], shoulder tendinopathies [11], knee osteoarthritis [12], and chronic neck pain [4,13]. A comparative study of their effect on the production of inflammatory cytokine IL-6 in mouse macrophage cells demonstrated that treatment with 0.7 mg/mL of CFAs produced a higher degree of reduction in IL-6 levels than 1 mM ibuprofen, 0.5 mM prednisone, or 0.5 mM piroxicam, demonstrating that CFAs may be considered valid alternatives to NSAIDs and steroids to counteract this type of inflammation without significant side effects [3].

CFAs are believed to exert their therapeutic effects through various mechanisms, including modulation of immune responses, lubrication of joints, and inhibition of inflammatory mediators. Nevertheless, while numerous products containing these compounds are currently available and widely used, their exact mechanism of action still remains incompletely understood. A mechanism proposed in 1994 suggested that CFAs exert their effects by stabilizing cell membranes and protecting synovial tissues [14]. These actions help maintain normal joint flexibility and mobility, alleviate pain, and enhance the production of joint fluid, thereby supporting proper lubrication [9,11,14]. However, more specific molecular targets that explain their mechanism of action have not yet been identified.

Over the past few years, the endocannabinoid system (ECS) has emerged as a critical regulator of numerous physiological and pathological processes, including pain modulation, inflammation, neuroprotection, and metabolic homeostasis [15,16], offering potential

therapeutic targets for managing several conditions. The ECS is a complex signalling network where the enzymes fatty-acid amide hydrolase (FAAH) and monoacylglycerol lipase (MAGL) play critical roles in terminating endocannabinoid signalling. FAAH catalyses the hydrolysis of amide-type endocannabinoids, such as anandamide and other *N*-acylethanolamides. On the other hand, MAGL promotes the hydrolysis of ester-type substrates, such as 2-arachidonoylglycerol (2-AG), the most abundant endocannabinoid ligand, into arachidonic acid and glycerol. This activity not only regulates 2-AG levels but also contributes to the biosynthesis of pro-inflammatory prostaglandins via arachidonic acid metabolism [17,18]. Emerging evidence has highlighted the therapeutic potential of MAGL inhibition in a variety of disorders, particularly those involving chronic pain and neuroinflammation [19–23]. The inhibition of MAGL elevates endogenous 2-AG levels, leading to enhanced activation of cannabinoid receptors CB1 and CB2, which are known to mediate analgesic and anti-inflammatory effects [24]. Moreover, by limiting the availability of arachidonic acid for cyclooxygenase pathways, MAGL inhibitors may simultaneously reduce pro-inflammatory eicosanoid production, providing a dual therapeutic effect [18,25].

Numerous academic institutions and pharmaceutical companies have worked on the development of MAGL inhibitors, employing both reversible and irreversible mechanisms of action [26–33]. While irreversible MAGL inhibitors often demonstrate strong inhibitory potency, their primary limitation lies in the side effects observed during *in vivo* studies [27,34]. Prolonged elevation of 2-AG levels resulting from their use can lead to CB1 receptor desensitization. Additionally, studies on mice treated with irreversible MAGL inhibitors or genetically lacking MAGL have revealed disrupted CB1-mediated synaptic plasticity, cross-tolerance to external CB1 agonists, and signs of physical dependence [27,34].

Recent studies have demonstrated that reversible MAGL inhibitors offer a promising strategy for nociceptive pain management with reduced risks of side effects associated with irreversible inhibitors, such as the compensatory upregulation of MAGL or off-target toxicities [21,24,25,35–41]. The development of potent, selective, and reversible MAGL inhibitors has therefore become an area of active research, with the goal of harnessing their nociceptive properties for clinical applications.

The aim of this article is to support the involvement of the ECS in the mechanism of action of CFAs and to discuss potential challenges and future directions for research in this field.

Considering the molecular structures of CFAs and their partial similarities to portions of some ester-based endocannabinoids (for example, 2-AG, virodhamine, etc.), we were intrigued by the possibility that they could act as false substrates in the enzyme that is primarily responsible for their degradation, MAGL, and that they could act as inhibitors of this enzyme, thus producing their final effects through an ECS-mediated mechanism. Therefore, we planned to obtain pure representative CFAs and to test the activity of each of them on the isolated human MAGL (*h*MAGL) enzyme, with the purpose of determining whether the reported local analgesic and anti-inflammatory activity of these compounds could be in part attributed to MAGL inhibition. At the same time, the aim of our work also included the identification of which of these CFAs displays the highest MAGL inhibition potency.

## 2. Materials and Methods

### 2.1. Chemical Synthesis: Materials and General Procedures

All chemicals and solvents were utilized as obtained from commercial sources without further purification. Purifications by means of chromatographic techniques were achieved on silica gel columns by flash chromatography (Kieselgel 40, 0.040–0.063 mm; Merck, Darmstadt, Germany). The reaction outcomes were monitored by thin layer chromatography (TLC) on Merck aluminium silica gel (60 F254) sheets and spots were detected under a

UV lamp. Solvent removal was performed in vacuo (rotating evaporator).  $\text{Na}_2\text{SO}_4$  was the drying agent utilized in all the procedures. Proton ( $^1\text{H}$ ) and carbon ( $^{13}\text{C}$ ) NMR spectra were obtained with a Bruker (Billerica, Massachusetts) Avance III 400 MHz spectrometer using the indicated deuterated solvents. The values of the chemical shifts are reported as parts per million (ppm) ( $\delta$  relative to residual solvent peak for  $^1\text{H}$  and  $^{13}\text{C}$ ).  $^1\text{H}$ -NMR spectra are described in the following order: multiplicity and number of protons derived from integrations of the peak areas. Standard abbreviations were used to indicate the signal multiplicity: t = triplet and m = multiplet. The ESI-MS (Electrospray Mass Spectrometry) spectra were recorded by direct injection at a  $5\ \mu\text{L}\ \text{min}^{-1}$  flow rate in an Orbitrap high-resolution mass spectrometer (Thermo, San Jose, CA, USA), provided with a HESI (Heated Electrospray Ionization) source under the following working conditions: sheath gas set at 24, auxiliary gas set at 5 (arbitrary units), positive polarity, spray voltage of 3.4 kV, capillary temperature of  $290\ ^\circ\text{C}$ , and S-lens RF level 50. Xcalibur 4.2 software (Thermo) was used for acquisition and analysis. For spectra acquisition, a nominal resolution (at  $m/z$  200) of 140,000 was employed. The reaction yields referred to the amounts of isolated and purified products obtained in non-optimized procedures.

#### 2.1.1. General Procedure for the Formation of Final Compounds **3b,d,e**

In a two-neck round-bottom flask, flame-dried, and under an Argon atmosphere, commercially available decanoic acid **2b**, tetradecanoic acid **2d**, or palmitic acid **2e** (1.0 equiv. 0.82 mmol) was dissolved in anhydrous acetonitrile (2.5 mL). 1,1'-Carbonyldiimidazole (CDI) (1.0 equiv., 0.82 mmol) was then added, and the mixture was stirred and heated at  $50\ ^\circ\text{C}$  for 1 h. Subsequently, 1-hexadecanol **1** (1.00 equiv., 0.825 mmol) was added, and the mixture was heated at  $65\ ^\circ\text{C}$  for 3 h. After confirming the complete consumption of the starting material, water was added to the reaction mixture. The reaction mixture was extracted with ethyl acetate (3x), and the organic phase was washed with brine (1x), dried over  $\text{Na}_2\text{SO}_4$ , filtered, and concentrated under reduced pressure. The crude product was purified by silica gel column chromatography. Elution with *n*-hexane or *n*-hexane/ethyl acetate 95:5 afforded the desired esters **3b,d,e**.

**Hexadecyl decanoate 3b.** White solid; 21% yield from hexadecan-1-ol **1** and decanoic acid **2b**.  $^1\text{H}$ -NMR ( $\text{CDCl}_3$ )  $\delta$  (ppm): 0.87 (t, 6H,  $J = 6.8\ \text{Hz}$ ), 1.20–1.36 (m, 38H), 1.56–1.66 (m, 4H), 2.28 (t, 2H,  $J = 7.6\ \text{Hz}$ ), 4.05 (t, 2H,  $J = 6.7\ \text{Hz}$ ).  $^{13}\text{C}$ -NMR ( $\text{CDCl}_3$ )  $\delta$  (ppm): 14.23, 14.24, 22.80, 22.82, 25.18, 26.08, 28.81, 29.31, 29.40, 29.42, 29.50, 29.57, 29.67, 29.71, 29.79, 29.81, 29.83, 31.04, 32.00, 32.06, 34.57, 64.54, 174.15. HRMS:  $m/z$  for  $\text{C}_{26}\text{H}_{53}\text{O}_2$  [ $\text{M} + \text{H}$ ] $^+$  calculated: 397.40456, found: 397.40329.

**Hexadecyl tetradecanoate 3d.** White solid; 52% yield from hexadecan-1-ol **1** and tetradecanoic acid **2d**.  $^1\text{H}$ -NMR ( $\text{CDCl}_3$ )  $\delta$  (ppm): 0.88 (t, 6H,  $J = 6.9\ \text{Hz}$ ), 1.20–1.37 (m, 46H), 1.56–1.66 (m, 4H), 2.28 (t, 2H,  $J = 7.6\ \text{Hz}$ ), 4.05 (t, 2H,  $J = 6.7\ \text{Hz}$ ).  $^{13}\text{C}$ -NMR ( $\text{CDCl}_3$ )  $\delta$  (ppm): 14.26 (2C), 22.84, 25.19, 26.09, 28.81, 29.32, 29.43, 29.51, 29.63, 29.68, 29.73, 29.76, 29.81, 29.84, 32.08, 34.58, 64.55, 174.17. HRMS:  $m/z$  for  $\text{C}_{30}\text{H}_{60}\text{O}_2\text{Na}$  [ $\text{M} + \text{Na}$ ] $^+$  calculated: 475.44910, found: 475.44855.

**Hexadecyl pentadecanoate 3e.** White solid; 7% yield from hexadecan-1-ol **1** and palmitic acid **2e**.  $^1\text{H}$ -NMR ( $\text{CDCl}_3$ )  $\delta$  (ppm): 0.88 (t, 6H,  $J = 6.8\ \text{Hz}$ ), 1.19–1.37 (m, 50H), 1.56–1.66 (m, 4H), 2.29 (t, 2H,  $J = 7.5\ \text{Hz}$ ), 4.05 (t, 2H,  $J = 6.7\ \text{Hz}$ ).  $^{13}\text{C}$ -NMR ( $\text{CDCl}_3$ )  $\delta$  (ppm): 14.28 (2C), 22.86 (2C), 25.21, 26.11, 28.82, 29.33, 29.43, 29.44, 29.53, 29.65, 29.70, 29.75, 29.77, 29.82, 29.86, 31.75, 32.09, 34.60, 64.57, 174.20. HRMS:  $m/z$  for  $\text{C}_{32}\text{H}_{64}\text{O}_2\text{Na}$  [ $\text{M} + \text{Na}$ ] $^+$  calculated: 503.48040, found: 503.47985.

### 2.1.2. General Procedure for the Formation of Final Compounds **3a,c,f–i**

In a two-neck round-bottom flask, flame-dried, and under an Argon atmosphere, commercially available hexanoic acid **2a**, dodecanoic acid **2c**, stearic acid **2f**, (*Z*)-tetradec-9-enoic acid **2g**, (*Z*)-hexadec-9-enoic acid **2h**, or oleic acid **2i** (1.0 equiv., 0.37 mmol) was dissolved in anhydrous dimethylformamide (1.8 mL) under stirring. Subsequently, 1-ethyl-3-(3-dimethylaminopropyl)carbodiimide (EDCI) (1.1 equiv., 0.41 mmol) and hydroxybenzotriazole (HOBt) (1.1 equiv., 0.41 mmol) were added. After 15 min, 1-hexadecanol **1** (1.1 equiv., 0.41 mmol) and diisopropylethylamine (DIPEA, 1.1 equiv., 0.41 mmol) were added. The mixture was stirred overnight at room temperature. Upon confirming the complete consumption of the starting material, the reaction mixture was extracted with ethyl acetate (3x), and the organic phase was washed with brine (2x), dried over Na<sub>2</sub>SO<sub>4</sub>, filtered, and concentrated under reduced pressure. The crude product was purified by silica gel column chromatography using a *n*-hexane/ethyl acetate mixture 95:5 as the eluent, yielding the desired esters **3a,c,f–i**.

**Hexadecyl hexanoate 3a.** Colourless oil; 39% yield from hexadecan-1-ol **1** and hexanoic acid **2a**. <sup>1</sup>H-NMR (CDCl<sub>3</sub>) δ (ppm): 0.88 (q, 6H, *J* = 6.7 Hz), 1.22–1.37 (m, 30H), 1.57–1.67 (m, 4H), 2.29 (t, 2H, *J* = 7.6 Hz), 4.05 (t, 2H, *J* = 6.8 Hz). <sup>13</sup>C-NMR (CDCl<sub>3</sub>) δ (ppm): 14.06, 14.26, 22.47, 22.84, 24.86, 26.08, 28.79, 29.40, 29.51, 29.67, 29.71, 29.79, 29.80, 29.81, 29.84, 31.47, 32.07, 34.52, 64.55, 174.17. HRMS: *m/z* for C<sub>22</sub>H<sub>45</sub>O<sub>2</sub> [M + H]<sup>+</sup> calculated: 341.34196, found: 341.34141.

**Hexadecyl dodecanoate 3c.** White solid; 35% yield from hexadecan-1-ol **1** and dodecanoic acid **2c**. <sup>1</sup>H-NMR (CDCl<sub>3</sub>) δ (ppm): 0.88 (t, 6H, *J* = 6.8 Hz), 1.20–1.37 (m, 42H), 1.56–1.66 (m, 4H), 2.28 (t, 2H, *J* = 7.6 Hz), 4.05 (t, 2H, *J* = 6.7 Hz). <sup>13</sup>C-NMR (CDCl<sub>3</sub>) δ (ppm): 14.26, 22.84, 25.19, 26.10, 28.82, 29.32, 29.41, 29.43, 29.49, 29.51, 29.62, 29.68, 29.73, 29.76, 29.80, 29.83, 29.85, 32.07, 32.08, 34.58, 64.55, 174.17. HRMS: *m/z* for C<sub>28</sub>H<sub>60</sub>O<sub>2</sub>N [M + NH<sub>4</sub>]<sup>+</sup> calculated: 442.46241, found: 442.46186.

**Hexadecyl stearate 3f.** White solid; 63% yield from hexadecan-1-ol **1** and stearic acid **2f**. <sup>1</sup>H-NMR (CDCl<sub>3</sub>) δ (ppm): 0.88 (t, 6H, *J* = 6.8 Hz), 1.19–1.37 (m, 54H), 1.56–1.66 (m, 4H), 2.28 (t, 2H, *J* = 7.5 Hz), 4.05 (t, 2H, *J* = 6.7 Hz). <sup>13</sup>C-NMR (CDCl<sub>3</sub>) δ (ppm): 14.23, 22.81, 25.15, 26.06, 28.77, 29.28, 29.37, 29.39, 29.41, 29.48, 29.59, 29.64, 29.70, 29.72, 29.77, 29.81, 32.04, 34.54, 64.52, 174.15. HRMS: *m/z* for C<sub>34</sub>H<sub>68</sub>O<sub>2</sub>Na [M + Na]<sup>+</sup> calculated: 531.51170, found: 531.51115.

**Hexadecyl (*Z*)-tetradec-9-enoate 3g.** Colourless oil; 49% yield from hexadecan-1-ol **1** and (*Z*)-tetradec-9-enoic acid **2g**. <sup>1</sup>H-NMR (CDCl<sub>3</sub>) δ (ppm): 0.85–0.92 (m, 6H), 1.20–1.37 (m, 38H), 1.56–1.66 (m, 4H), 1.98–2.05 (m, 4H), 2.29 (t, 2H, *J* = 7.5 Hz), 4.05 (t, 2H, *J* = 6.7 Hz), 5.29–5.39 (m, 2H). <sup>13</sup>C-NMR (CDCl<sub>3</sub>) δ (ppm): 14.14, 14.26, 22.49, 22.84, 25.17, 26.09, 27.07, 27.30, 28.81, 29.25, 29.28, 29.31, 29.41, 29.51, 29.68, 29.73, 29.81, 29.84, 32.08, 32.11, 34.56, 64.56, 129.92, 130.08, 174.15. HRMS: *m/z* for C<sub>30</sub>H<sub>59</sub>O<sub>2</sub> [M + H]<sup>+</sup> calculated: 451.45151, found: 451.45096.

**Hexadecyl (*Z*)-hexadec-9-enoate 3h.** Colourless oil; 53% yield from hexadecan-1-ol **1** and (*Z*)-hexadec-9-enoic acid **2h**. <sup>1</sup>H-NMR (CDCl<sub>3</sub>) δ (ppm): 0.88 (m, 6H), 1.20–1.38 (m, 42H), 1.56–1.66 (m, 4H), 1.97–2.05 (m, 4H), 2.29 (t, 2H, *J* = 7.5 Hz), 4.05 (t, 2H, *J* = 6.7 Hz), 5.29–5.39 (m, 2H). <sup>13</sup>C-NMR (CDCl<sub>3</sub>) δ (ppm): 14.24, 14.26, 22.80, 22.83, 25.16, 26.08, 27.30, 27.36, 28.80, 29.13, 29.25, 29.27, 29.31, 29.40, 29.50, 29.67, 29.72, 29.79, 29.82, 29.83, 29.88, 31.93, 32.06, 34.55, 64.55, 129.90, 130.13, 174.14. HRMS: *m/z* for C<sub>32</sub>H<sub>63</sub>O<sub>2</sub> [M + H]<sup>+</sup> calculated: 479.48281, found: 479.48145.

**Hexadecyl oleate 3i.** Colourless oil; 51% yield from hexadecan-1-ol **1** and oleic acid **2i**. <sup>1</sup>H-NMR (CDCl<sub>3</sub>) δ (ppm): 0.88 (t, 6H, *J* = 6.8 Hz), 1.20–1.38 (m, 46H), 1.57–1.66 (m, 4H), 1.97–2.06 (m, 4H), 2.19 (t, 2H, *J* = 7.5 Hz), 4.05 (t, 2H, *J* = 6.7 Hz), 5.29–5.39 (m, 2H). <sup>13</sup>C-NMR (CDCl<sub>3</sub>) δ (ppm): 14.26, 22.85, 25.18, 26.11, 27.33, 27.38, 28.83, 29.27, 29.30, 29.33,

29.42, 29.48, 29.52, 29.69, 29.74, 29.82, 29.86, 29.93, 32.07, 32.09, 34.57, 64.57, 129.91, 130.15, 174.14. HRMS:  $m/z$  for  $C_{34}H_{70}O_2N$   $[M + NH_4]^+$  calculated: 524.54066, found: 524.54011.

## 2.2. MAGL Inhibition Assays

Human recombinant MAGL and 4-nitrophenyl acetate (4-NPA) were purchased from Cayman Chemical. *h*MAGL had a  $\geq 95\%$  purity rate estimated by SDS-PAGE and was stored at  $-80^\circ\text{C}$  in order to preserve its stability, as recommended by the producer.  $IC_{50}$  values were determined using 96-well microtiter plates. The enzymatic reaction was conducted at room temperature in a final volume of 200  $\mu\text{L}$ , prepared in 10 mM Tris buffer (pH 7.2) containing 1 mM EDTA and 0.1 mg/mL bovine serum albumin (BSA). A volume of 150  $\mu\text{L}$  of 4-NPA at 133.3  $\mu\text{M}$  was mixed with 10  $\mu\text{L}$  of dimethylsulfoxide (DMSO) containing the desired concentration of the tested compound. The reaction was initiated by adding 40  $\mu\text{L}$  of MAGL (11 ng per well), ensuring linearity over 30 min. The reference inhibitor JZL-184 [28] was used as a positive control. Initially, CFAs were tested at a single concentration of 50  $\mu\text{M}$ , and the single-point percentage of inhibition was determined. Subsequently, the compound exhibiting the highest single-point percentage inhibition, compound **3b**, was further evaluated to determine its  $IC_{50}$  value. The final concentrations of the tested compound **3b** ranged from 50  $\mu\text{M}$  to 0.78  $\mu\text{M}$ . After 30 min, absorbance was measured at 405 nm using a Victor X3 Microplates Reader (PerkinElmer®, Shelton, Connecticut,). The control reactions included one without the test compound and another without both the compound and MAGL. The final data were obtained from duplicate measurements of three independent experiments. The spectrophotometric data were analysed and interpreted using the GraphPad Prism software, version 10.2.0. The data are presented as an average of 3 replicates (mean  $\pm$  standard deviation), and a statistical analysis was performed using GraphPad Prism software. The  $IC_{50}$  value was calculated using the Sigmoidal dose-response fitting in GraphPad Prism software. To eliminate potential false positives, a blank analysis was carried out at each compound concentration. The final absorbance values were corrected by subtracting the absorbance measured in the absence of MAGL under identical conditions.

## 3. Results

### 3.1. Chemistry

We synthesized and purified nine CFAs **3a–i** (Figure 2). This series includes those that are commonly utilized in topical formulations, often as mixtures, containing both saturated (**3c–e**) and unsaturated fatty acid portions (**3g–i**), along with three additional analogues of the saturated series (**3a,b,f**), which were included to probe the effect of the length of the acyl chain on the MAGL inhibition properties of these compounds. The synthesis for obtaining compounds **3a–i** is outlined in Figure 3 and involves a rapid, single-step procedure based on the condensation of commercially available cetyl alcohol (**1**) with the respective commercially available carboxylic acids (**2a–i**), yielding the desired CFAs (**3a–i**) with variable yields.

Initially, commercially available cetyl alcohol (**1**) was condensed with the respective commercially available carboxylic acids **2b,d,e** in the presence of carbonyldiimidazole (CDI) as the coupling agent, using anhydrous acetonitrile ( $\text{CH}_3\text{CN}$ ) as the solvent and heating at  $80^\circ\text{C}$  for three hours. This procedure yielded the first CFAs **3b,d,e** with moderate to good yields.

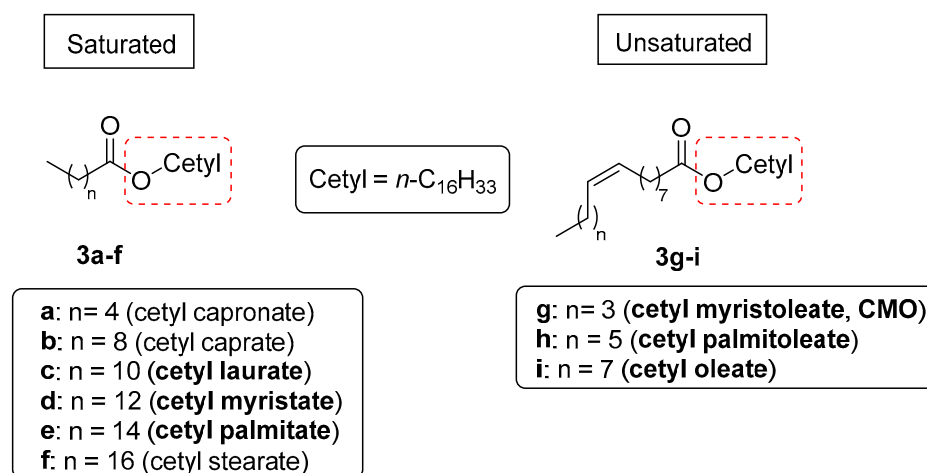


**Figure 2.** Structures of the synthesized CFAs **3a–i**. The cetyl portion is highlighted in the red dashed square. The names of CFAs commonly present in marketed topic formulations are highlighted in bold.

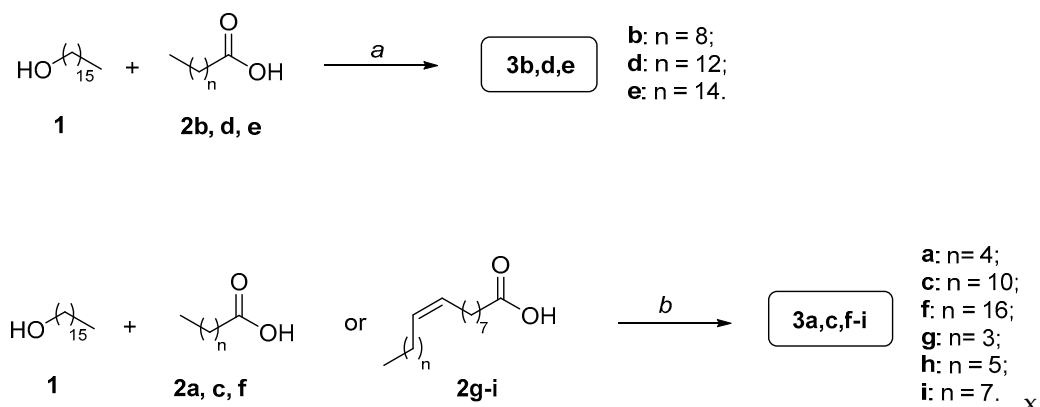


**Figure 3.** Synthesis of CFAs **3a–i**. Reagents and conditions: (a) CDI, anhydrous  $\text{CH}_3\text{CN}$ ,  $80^\circ\text{C}$ , 3 h [7–52%]; (b) EDCI, HOBt, DIPEA, anhydrous DMF, rt, 12 h [35–63%].

To enhance the reaction yields, the synthesis of the remaining CFAs was carried out under modified conditions. Based on literature precedents, commercially available cetyl alcohol **1** was condensed with the respective carboxylic acids **2a,c,f–i** in the presence of 1-ethyl-3-(3-dimethylaminopropyl)carbodiimide (EDCI) as the coupling agent, hydroxybenzotriazole (HOBt) as an activated ester, *N,N*-diisopropylethylamine (DIPEA) as the base, and anhydrous dimethylformamide (DMF) as the solvent, at room temperature for 12 h. This optimized procedure afforded the remaining desired final compounds **3a,c,f–i** with good to optimal yields.  $^1\text{H}$  and  $^{13}\text{C}$  NMR spectra of the final compounds **3a–i** (Figures S1–S9) can be found in the Supplementary Material.

### 3.2. Enzymatic Inhibition Assays

A spectrophotometric assay, in which 4-nitrophenylacetate was used as the enzyme substrate, was conducted to test the *h*MAGL inhibition activities of the newly synthesized CFAs. The percentages of MAGL enzyme inhibition are reported in Figure 4. The final compounds **3a–i** were tested at a single concentration of  $50\ \mu\text{M}$ . Among these compounds, **3b** exhibited the highest single-point inhibition percentage (47.1%). For this compound, a full dose–response curve was obtained to calculate its  $\text{IC}_{50}$  value, which turned out to be  $36 \pm 4\ \mu\text{M}$ , representing the mean of three independent experiments conducted in duplicate.



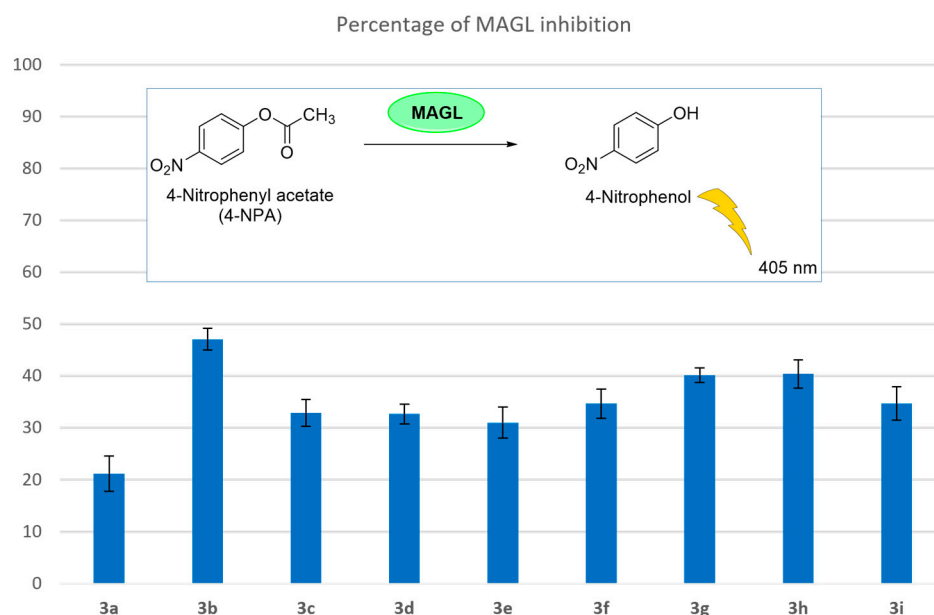


**Figure 4.** In vitro inhibitory activity (%) on *h*MAGL of derivatives **3a–i**.

#### 4. Discussion

It is important to note that all the CFAs tested showed some degree of MAGL inhibition, although there are significant differences to consider. First of all, the series of unsaturated CFAs (**3g–i**) generally display higher potencies than most of the saturated derivatives. In particular, compound **3g** that corresponds to CMO, whose anti-arthritis properties had been previously demonstrated in murine models [2], proved to efficiently inhibit MAGL. Similarly, its close analogue **3h** (cetyl palmitoleate), possessing the double bond at the same distance from the ester group as **3g**, proved to be equally active, whereas their longer analogue **3i** (cetyl oleate) displayed slightly weaker potency in the same test, probably due to the extended length of its acyl chain encountering some steric clash with the enzyme active site.

Overall, the series of  $\Delta 9$ -unsaturated fatty acid esters demonstrated that an acyl chain content of 14 to 16 carbon atoms leads to the formation of more potent inhibitors (**3g,h**) than 18 carbon atoms (**3i**).

A different behaviour was observed in the saturated series of CFAs, which are generally weaker inhibitors, with the single exception of compound **3b** (cetyl caproate or decanoate), which proved to be the most potent inhibitor of the whole set of CFAs described here. In this case, the optimal length of the acyl chain turned out to be 10 carbon atoms, as shorter (**3a**) or longer saturated acyl groups (**3c–f**) produced weaker MAGL inhibitors. Different optimal lengths between the unsaturated vs. saturated derivatives might be ascribed to the distinct conformational freedom of their respective side chains, which may strongly affect their spatial disposition. A full dose–response curve was obtained for the most active inhibitor, **3b**, and its  $IC_{50}$  value turned out to be 36  $\mu M$ , which of course does not represent extremely potent inhibition, especially when compared to other MAGL inhibitors reported in the literature that display activities in the low/sub-nanomolar range. We are aware that these compounds are characterized by weaker potencies when compared to other synthetic MAGL inhibitors reported in the literature [42]. However, a concentration in the micromolar range of **3b** and its close analogues is expected to be readily achieved in musculoskeletal compartments by topical application, thanks to efficient passive absorption through the skin due to the highly lipophilic nature of these compounds. Therefore, we strongly believe that MAGL inhibition levels caused by these CFAs significantly contribute to the overall clinical effectiveness of their preparations. A clear advantage of these CFAs over more



potent synthetic MAGL inhibitors is the fact that they are naturally available biomolecules that have been extensively utilized during the past decades in topical formulations to treat musculoskeletal afflictions, and no evident toxicities have so far emerged from their use.

Overall, we think that our findings lay the groundwork for the development and clinical use of small molecules that are able to indirectly activate cannabimimetic pathways to produce a local analgesic and anti-inflammatory effect. This strategy would represent a clear advantage over NSAIDs, which are known to produce gastrointestinal side effects, as well as over opioid analgesic, which instead pose a serious risk of addiction and dependence.

## 5. Conclusions

Taken together, these results provide promising evidence supporting the hypothesis that the analgesic effects of CFAs may be mediated, at least in part, by MAGL inhibition. This potential mechanism offers a novel perspective on the therapeutic applications of CFAs, positioning them as promising candidates for pain management strategies locally targeting the endocannabinoid system. This would not be the first example of the unexpected involvement of cannabinoid mechanisms in widely utilized drugs, such as in the case of a mild analgesic drug, paracetamol [43].

Furthermore, this work may indicate which CFA could be more effective based on this mechanism of action and, therefore, guide companies to optimize the composition of their products. Finally, our results demonstrate that the most potent MAGL inhibitor of this series, cetyl caprate **3b**, which, to the best of our knowledge, is not commonly employed in CFA-based formulations, might potentially induce a more efficient therapeutic outcome and should instead be included in these products. Of course, further investigations are necessary to validate these results, including more in-depth pharmacological evaluations of this class of compounds. Meanwhile, it appears evident that therapeutic interventions producing local cannabimimetic effects may represent novel strategies that can lead to the development of new clinical candidates, with the aim of producing more effective and safer drugs against musculoskeletal afflictions.

**Supplementary Materials:** The following supporting information can be downloaded at <https://www.mdpi.com/article/10.3390/biom15030363/s1>, Figure S1:  $^1\text{H}$ -NMR and  $^{13}\text{C}$ -NMR of compound **3a**; Figure S2:  $^1\text{H}$ -NMR and  $^{13}\text{C}$ -NMR of compound **3b**; Figure S3:  $^1\text{H}$ -NMR and  $^{13}\text{C}$ -NMR of compound **3c**; Figure S4:  $^1\text{H}$ -NMR and  $^{13}\text{C}$ -NMR of compound **3d**; Figure S5:  $^1\text{H}$ -NMR and  $^{13}\text{C}$ -NMR of compound **3e**; Figure S6:  $^1\text{H}$ -NMR and  $^{13}\text{C}$ -NMR of compound **3f**; Figure S7:  $^1\text{H}$ -NMR and  $^{13}\text{C}$ -NMR of compound **3g**; Figure S8:  $^1\text{H}$ -NMR and  $^{13}\text{C}$ -NMR of compound **3h**; Figure S9:  $^1\text{H}$ -NMR and  $^{13}\text{C}$ -NMR of compound **3i**.

**Author Contributions:** Conceptualization, C.G. and F.M.; methodology, G.B. and C.G.; validation, G.B. and C.G.; formal analysis, G.B., C.G., T.T. and F.M.; investigation, G.B. and C.G.; resources, C.G. and F.M.; data curation, G.B.; writing—original draft preparation, G.B. and F.M.; writing—review and editing, G.B., C.G., T.T. and F.M.; visualization, C.G., T.T. and F.M.; supervision, C.G. and F.M. All authors have read and agreed to the published version of the manuscript.

**Funding:** This research received no external funding.

**Institutional Review Board Statement:** Not applicable.

**Informed Consent Statement:** Not applicable.

**Data Availability Statement:** The original contributions presented in this study are included in the article/Supplementary Materials. Further inquiries can be directed to the corresponding author(s).

**Acknowledgments:** The authors thank Eleonora Gori for her technical support in the chemical synthesis and Beatrice Muscatello for the HRMS analysis of the final products.

**Conflicts of Interest:** The authors declare no conflicts of interest.

## Abbreviations

The following abbreviations are used in this manuscript:

CFA	Cetylated Fatty Acid
AEA	Anandamide
2-AG	2-Arachidonoylglycerol
MAGL	Monoacylglycerol Lipase
NSAIDs	Nonsteroidal Anti-Inflammatory Drugs
CMO	Cetyl Myristoleate
ECS	Endocannabinoid System
HESI	Heated Electrospray Ionization
ES-MS	Electrospray Mass Spectrometry
DMSO	Dimethylsulfoxide

## References

1. Machado, G.C.; Abdel-Shaheed, C.; Underwood, M.; Day, R.O. Non-Steroidal Anti-Inflammatory Drugs (NSAIDs) for Musculoskeletal Pain. *BMJ* **2021**, *372*, n104. [[CrossRef](#)] [[PubMed](#)]
2. Hunter, K.W.; Gault, R.A.; Stehouwer, J.S.; Tam-Chang, S.-W. Synthesis of Cetyl Myristoleate and Evaluation of Its Therapeutic Efficacy in a Murine Model of Collagen-Induced Arthritis. *Pharmacol. Res.* **2003**, *47*, 43–47. [[CrossRef](#)] [[PubMed](#)]
3. Hudita, A.; Galateanu, B.; Dinescu, S.; Costache, M.; Dinischiotu, A.; Negrei, C.; Stan, M.; Tsatsakis, A.; Nikitovic, D.; Lupuliasa, D.; et al. In Vitro Effects of Cetylated Fatty Acids Mixture from Celadrin on Chondrogenesis and Inflammation with Impact on Osteoarthritis. *Cartilage* **2020**, *11*, 88–97. [[CrossRef](#)] [[PubMed](#)]
4. Izzo, R.; Rossato, M.; Tarantino, G.; Mascolo, N.; Puleio, M. Effects of Esters' Cetylated Fatty Acids Taping for Chronic Neck Pain with Mobility Deficit in Patients with Breast Cancer. *Support. Care Cancer* **2023**, *31*, 20. [[CrossRef](#)]
5. Sjövall, P.; Skedung, L.; Gregoire, S.; Biganska, O.; Clément, F.; Luengo, G.S. Imaging the Distribution of Skin Lipids and Topically Applied Compounds in Human Skin Using Mass Spectrometry. *Sci. Rep.* **2018**, *8*, 16683. [[CrossRef](#)]
6. Kraemer, W.J.; Ratamess, N.A.; Maresh, C.M.; Anderson, J.A.; Tiberio, D.P.; Joyce, M.E.; Messinger, B.N.; French, D.N.; Sharman, M.J.; Rubin, M.R.; et al. Effects of Treatment with a Cetylated Fatty Acid Topical Cream on Static Postural Stability and Plantar Pressure Distribution in Patients with Knee Osteoarthritis. *J. Strength Cond. Res.* **2005**, *19*, 115. [[CrossRef](#)]
7. Kraemer, W.J.; Ratamess, N.A.; Maresh, C.M.; Anderson, J.A.; Volek, J.S.; Tiberio, D.P.; Joyce, M.E.; Messinger, B.N.; French, D.N.; Sharman, M.J.; et al. A Cetylated Fatty Acid Topical Cream with Menthol Reduces Pain and Improves Functional Performance in Individuals with Arthritis. *J. Strength Cond. Res.* **2005**, *19*, 475. [[CrossRef](#)]
8. Kraemer, W.J.; Ratamess, N.A.; Anderson, J.M.; Maresh, C.M.; Tiberio, D.P.; Joyce, M.E.; Messinger, B.N.; French, D.N.; Rubin, M.R.; Gómez, A.L.; et al. Effect of a Cetylated Fatty Acid Topical Cream on Functional Mobility and Quality of Life of Patients with Osteoarthritis. *J. Rheumatol.* **2004**, *31*, 767–774.
9. Hesslink, R.; Armstrong, D.; Nagendran, M.V.; Sreevatsan, S.; Barathur, R. Cetylated Fatty Acids Improve Knee Function in Patients with Osteoarthritis. *J. Rheumatol.* **2002**, *29*, 1708–1712.
10. Pampaloni, E.; Pera, E.; Maggi, D.; Lucchinelli, R.; Chiappino, D.; Costa, A.; Venturini, V.; Tarantino, G. Association of Cetylated Fatty Acid Treatment with Physical Therapy Improves Athletic Pubalgia Symptoms in Professional Roller Hockey Players. *Heliyon* **2020**, *6*, e04526. [[CrossRef](#)]
11. Lanzisera, R.; Baroni, A.; Lenti, G.; Geri, E. A Prospective Observational Study on the Beneficial Effects and Tolerability of a Cetylated Fatty Acids (CFA) Complex in a Patch Formulation for Shoulder Tendon Disorders. *BMC Musculoskelet. Disord.* **2022**, *23*, 352. [[CrossRef](#)] [[PubMed](#)]
12. Ariani, A. Short-Term Effect of Topical Cetylated Fatty Acid on Early and Advanced Knee Osteoarthritis: A Multi-Center Study. *Arch. Rheumatol.* **2018**, *33*, 438–442. [[CrossRef](#)]
13. Sharan, D.; Jacob, B.N.; Ajeesh, P.S.; Bookout, J.B.; Barathur, R.R. The Effect of Cetylated Fatty Esters and Physical Therapy on Myofascial Pain Syndrome of the Neck. *J. Bodyw. Mov. Ther.* **2011**, *15*, 363–374. [[CrossRef](#)]
14. Diehl, H.W.; May, E.L. Cetyl Myristoleate Isolated from Swiss Albino Mice: An Apparent Protective Agent against Adjuvant Arthritis in Rats. *J. Pharm. Sci.* **1994**, *83*, 296–299. [[CrossRef](#)] [[PubMed](#)]
15. Di Marzo, V. The Endocannabinoid System: Its General Strategy of Action, Tools for Its Pharmacological Manipulation and Potential Therapeutic Exploitation. *Pharmacol. Res.* **2009**, *60*, 77–84. [[CrossRef](#)] [[PubMed](#)]

16. De Petrocellis, L.; Di Marzo, V. An Introduction to the Endocannabinoid System: From the Early to the Latest Concepts. *Best Pract. Res. Clin. Endocrinol. Metab.* **2009**, *23*, 1–15. [\[CrossRef\]](#)
17. Blankman, J.L.; Cravatt, B.F. Chemical Probes of Endocannabinoid Metabolism. *Pharmacol. Rev.* **2013**, *65*, 849–871. [\[CrossRef\]](#)
18. Nomura, D.K.; Morrison, B.E.; Blankman, J.L.; Long, J.Z.; Kinsey, S.G.; Marcondes, M.C.G.; Ward, A.M.; Hahn, Y.K.; Lichtman, A.H.; Conti, B.; et al. Endocannabinoid Hydrolysis Generates Brain Prostaglandins That Promote Neuroinflammation. *Science* **2011**, *334*, 809–813. [\[CrossRef\]](#)
19. Mulvihill, M.M.; Nomura, D.K. Therapeutic Potential of Monoacylglycerol Lipase Inhibitors. *Life Sci.* **2013**, *92*, 492–497. [\[CrossRef\]](#)
20. Guindon, J.; Desroches, J.; Beaulieu, P. The Antinociceptive Effects of Intraplantar Injections of 2-Arachidonoyl Glycerol Are Mediated by Cannabinoid CB2 Receptors. *Br. J. Pharmacol.* **2007**, *150*, 693–701. [\[CrossRef\]](#)
21. Kinsey, S.G.; Long, J.Z.; O’Neal, S.T.; Abdullah, R.A.; Poklis, J.L.; Boger, D.L.; Cravatt, B.F.; Lichtman, A.H. Blockade of Endocannabinoid-Degrading Enzymes Attenuates Neuropathic Pain. *J. Pharmacol. Exp. Ther.* **2009**, *330*, 902–910. [\[CrossRef\]](#) [\[PubMed\]](#)
22. Griebel, G.; Pichat, P.; Beeské, S.; Leroy, T.; Redon, N.; Jacquet, A.; Françon, D.; Bert, L.; Even, L.; Lopez-Grancha, M.; et al. Selective Blockade of the Hydrolysis of the Endocannabinoid 2-Arachidonoylglycerol Impairs Learning and Memory Performance While Producing Antinociceptive Activity in Rodents. *Sci. Rep.* **2015**, *5*, 7642. [\[CrossRef\]](#)
23. Woodhams, S.; Wong, A.; Barrett, D.; Bennett, A.; Chapman, V.; Alexander, S. Spinal Administration of the Monoacylglycerol Lipase Inhibitor JZL184 Produces Robust Inhibitory Effects on Nociceptive Processing and the Development of Central Sensitization in the Rat. *Br. J. Pharmacol.* **2012**, *167*, 1609–1619. [\[CrossRef\]](#)
24. Gil-Ordóñez, A.; Martín-Fontecha, M.; Ortega-Gutiérrez, S.; López-Rodríguez, M.L. Monoacylglycerol Lipase (MAGL) as a Promising Therapeutic Target. *Biochem. Pharmacol.* **2018**, *157*, 18–32. [\[CrossRef\]](#)
25. Viader, A.; Ogasawara, D.; Joslyn, C.M.; Sanchez-Alavez, M.; Mori, S.; Nguyen, W.; Conti, B.; Cravatt, B.F. A Chemical Proteomic Atlas of Brain Serine Hydrolases Identifies Cell Type-Specific Pathways Regulating Neuroinflammation. *eLife* **2016**, *5*, e12345. [\[CrossRef\]](#)
26. Ghosh, S.; Wise, L.E.; Chen, Y.; Gujjar, R.; Mahadevan, A.; Cravatt, B.F.; Lichtman, A.H. The Monoacylglycerol Lipase Inhibitor JZL184 Suppresses Inflammatory Pain in the Mouse Carrageenan Model. *Life Sci.* **2013**, *92*, 498–505. [\[CrossRef\]](#) [\[PubMed\]](#)
27. Schlosburg, J.E.; Kinsey, S.G.; Ignatowska-Jankowska, B.; Ramesh, D.; Abdullah, R.A.; Tao, Q.; Booker, L.; Long, J.Z.; Selley, D.E.; Cravatt, B.F.; et al. Prolonged Monoacylglycerol Lipase Blockade Causes Equivalent Cannabinoid Receptor Type 1 Receptor-Mediated Adaptations in Fatty Acid Amide Hydrolase Wild-Type and Knockout Mice. *J. Pharmacol. Exp. Ther.* **2014**, *350*, 196–204. [\[CrossRef\]](#)
28. Long, J.Z.; Li, W.; Booker, L.; Burston, J.J.; Kinsey, S.G.; Schlosburg, J.E.; Pavón, F.J.; Serrano, A.M.; Selley, D.E.; Parsons, L.H.; et al. Selective Blockade of 2-Arachidonoylglycerol Hydrolysis Produces Cannabinoid Behavioral Effects. *Nat. Chem. Biol.* **2009**, *5*, 37–44. [\[CrossRef\]](#) [\[PubMed\]](#)
29. King, A.R.; Dotsey, E.Y.; Lodola, A.; Jung, K.M.; Ghomian, A.; Qiu, Y.; Fu, J.; Mor, M.; Piomelli, D. Discovery of Potent and Reversible Monoacylglycerol Lipase Inhibitors. *Chem. Biol.* **2009**, *16*, 1045–1052. [\[CrossRef\]](#)
30. Chicca, A.; Marazzi, J.; Gertsch, J. The Antinociceptive Triterpene  $\beta$ -Amyrin Inhibits 2-Arachidonoylglycerol (2-AG) Hydrolysis without Directly Targeting Cannabinoid Receptors. *Br. J. Pharmacol.* **2012**, *167*, 1596–1608. [\[CrossRef\]](#)
31. Hernández-Torres, G.; Cipriano, M.; Hedén, E.; Björklund, E.; Canales, Á.; Zian, D.; Feliú, A.; Mecha, M.; Guaza, C.; Fowler, C.J.; et al. A Reversible and Selective Inhibitor of Monoacylglycerol Lipase Ameliorates Multiple Sclerosis. *Angew. Chemie Int. Ed.* **2014**, *53*, 13765–13770. [\[CrossRef\]](#) [\[PubMed\]](#)
32. Bononi, G.; Granchi, C.; Lapillo, M.; Giannotti, M.; Nieri, D.; Fortunato, S.; El Boustani, M.; Caligiuri, I.; Poli, G.; Carlson, K.E.; et al. Discovery of Long-Chain Salicylketoxime Derivatives as Monoacylglycerol Lipase (MAGL) Inhibitors. *Eur. J. Med. Chem.* **2018**, *157*, 817–836. [\[CrossRef\]](#)
33. Aida, J.; Fushimi, M.; Kusumoto, T.; Sugiyama, H.; Arimura, N.; Ikeda, S.; Sasaki, M.; Sogabe, S.; Aoyama, K.; Koike, T. Design, Synthesis, and Evaluation of Piperazinyl Pyrrolidin-2-Ones as a Novel Series of Reversible Monoacylglycerol Lipase Inhibitors. *J. Med. Chem.* **2018**, *61*, 9205–9217. [\[CrossRef\]](#) [\[PubMed\]](#)
34. Schlosburg, J.E.; Blankman, J.L.; Long, J.Z.; Nomura, D.K.; Pan, B.; Kinsey, S.G.; Nguyen, P.T.; Ramesh, D.; Booker, L.; Burston, J.J.; et al. Chronic Monoacylglycerol Lipase Blockade Causes Functional Antagonism of the Endocannabinoid System. *Nat. Neurosci.* **2010**, *13*, 1113–1119. [\[CrossRef\]](#)
35. Di Stefano, M.; Masoni, S.; Bononi, G.; Poli, G.; Galati, S.; Gado, F.; Manzi, S.; Vagaggini, C.; Brai, A.; Caligiuri, I.; et al. Design, Synthesis, ADME and Biological Evaluation of Benzylpiperidine and Benzylpiperazine Derivatives as Novel Reversible Monoacylglycerol Lipase (MAGL) Inhibitors. *Eur. J. Med. Chem.* **2024**, *263*, 115916. [\[CrossRef\]](#) [\[PubMed\]](#)
36. Granchi, C.; Bononi, G.; Ferrisi, R.; Gori, E.; Mantini, G.; Glasmacher, S.; Poli, G.; Palazzolo, S.; Caligiuri, I.; Rizzolio, F.; et al. Design, Synthesis and Biological Evaluation of Second-Generation Benzoylpiperidine Derivatives as Reversible Monoacylglycerol Lipase (MAGL) Inhibitors. *Eur. J. Med. Chem.* **2021**, *209*, 112857. [\[CrossRef\]](#)

37. Granchi, C.; Lapillo, M.; Glasmacher, S.; Bononi, G.; Licari, C.; Poli, G.; el Boustani, M.; Caligiuri, I.; Rizzolio, F.; Gertsch, J.; et al. Optimization of a Benzoylpiperidine Class Identifies a Highly Potent and Selective Reversible Monoacylglycerol Lipase (MAGL) Inhibitor. *J. Med. Chem.* **2019**, *62*, 1932–1958. [[CrossRef](#)]
38. Bononi, G.; Tonarini, G.; Poli, G.; Barravecchia, I.; Caligiuri, I.; Macchia, M.; Rizzolio, F.; Demontis, G.C.; Minutolo, F.; Granchi, C.; et al. Monoacylglycerol Lipase (MAGL) Inhibitors Based on a Diphenylsulfide-Benzoylpiperidine Scaffold. *Eur. J. Med. Chem.* **2021**, *223*, 113679. [[CrossRef](#)]
39. Bononi, G.; Di Stefano, M.; Poli, G.; Ortore, G.; Meier, P.; Masetto, F.; Caligiuri, I.; Rizzolio, F.; Macchia, M.; Chicca, A.; et al. Reversible Monoacylglycerol Lipase Inhibitors: Discovery of a New Class of Benzylpiperidine Derivatives. *J. Med. Chem.* **2022**, *65*, 7118–7140. [[CrossRef](#)]
40. Tuccinardi, T.; Granchi, C.; Rizzolio, F.; Caligiuri, I.; Battistello, V.; Toffoli, G.; Minutolo, F.; Macchia, M.; Martinelli, A. Identification and Characterization of a New Reversible MAGL Inhibitor. *Bioorg. Med. Chem.* **2014**, *22*, 3285–3291. [[CrossRef](#)]
41. Granchi, C.; Rizzolio, F.; Palazzolo, S.; Carmignani, S.; Macchia, M.; Saccomanni, G.; Manera, C.; Martinelli, A.; Minutolo, F.; Tuccinardi, T. Structural Optimization of 4-Chlorobenzoylpiperidine Derivatives for the Development of Potent, Reversible, and Selective Monoacylglycerol Lipase (MAGL) Inhibitors. *J. Med. Chem.* **2016**, *59*, 10299–10314. [[CrossRef](#)] [[PubMed](#)]
42. Kashyap, A.; Kumar, S.; Dutt, R. A Review on Structurally Diversified Synthesized Molecules as Monoacylglycerol Lipase Inhibitors and Their Therapeutic Uses. *Curr. Drug Res. Rev.* **2022**, *14*, 96–115. [[CrossRef](#)] [[PubMed](#)]
43. Högestätt, E.D.; Jönsson, B.A.G.; Ermund, A.; Andersson, D.A.; Björk, H.; Alexander, J.P.; Cravatt, B.F.; Basbaum, A.I.; Zygmunt, P.M. Conversion of Acetaminophen to the Bioactive *N*-Acylphenolamine AM404 via Fatty Acid Amide Hydrolase-Dependent Arachidonic Acid Conjugation in the Nervous System. *J. Biol. Chem.* **2005**, *280*, 31405–31412. [[CrossRef](#)] [[PubMed](#)]

**Disclaimer/Publisher’s Note:** The statements, opinions and data contained in all publications are solely those of the individual author(s) and contributor(s) and not of MDPI and/or the editor(s). MDPI and/or the editor(s) disclaim responsibility for any injury to people or property resulting from any ideas, methods, instructions or products referred to in the content.